REMOTE SENSING ALGORITHMS BY NUMERICAL INVERSION OF RADIATIVE TRANSFER MODELS: NEURAL NETWORK AND OPTIMIZATION METHODS COMPARED

D.C. Hughes[1], R.J. Holyer[1], and Z.P. Lee[2]

[1] University of Southern Mississippi, School of Mathematical Sciences, Bldg. 9313, Rm 113, Stennis Space Center, MS, USA, 39529
email: David.C.Hughes@usm.edu

[2] University of South Florida, Department of Marine Science
140 7th Ave. S., St. Petersburg, FL 33701

INTRODUCTION AND APPROACH

In ocean optics the forward problem (*i.e.*, given water optical properties and illumination conditions, find the water-leaving radiance) is solved and several computer implementations of in-water radiative transfer are available. Using these radiative transfer models, water-leaving radiance can be calculated with precision limited only by the availability of computer resources. However, the inverse problem (*i.e.*, given observations of water-leaving radiance, find the water and illumination conditions that necessarily lead to this observation) is not solved in closed analytical form. The inverse relationship may even be many-to-one. Moreover solution of the inverse problem is the essence of remote sensing, where the objective is retrieval of water depth, water inherent optical properties (IOPs), bottom reflectance (r_b), or some other parameter from observations of water-leaving spectral radiance or reflectance. In lieu of rigorous inversion, various empirical, semi-analytical, statistical, or numerical methods have been utilized for retrieval of ocean parameters from remotely sensed spectral radiance data. Two methods in particular have received recent attention. The methods are similar in many ways but quite different in implementation. Both methods have resulted in reasonable inversions of hyperspectral data. However, the two methods have never been applied to the same data set to allow quantitative comparisons. This paper presents the first comparison of this type. The methods are compared on the basis of accuracy, efficiency, robustness, and extension to complex coastal environments.

Both methods are based on radiative transfer models. Because the algorithms embody physics rather than statistical relationships, one would expect that both algorithms would be robust or universal in the sense that they would be applicable to many diverse water and bottom types. The first method (Lee *et al.,* (1999, 2001) solves the inverse problem by iteration in the forward direction. To provide an efficient forward calculation, a simplified forward radiative transfer model, the semi-analytical (SA) model, has been developed. The second algorithm uses a neural network (NN) trained using a large data set generated by HYDROLIGHT, a full forward radiative transfer model (Mobley, 1994), to produce a numerical inversion which takes the observed spectrum as input and generates a depth value or IOP value as output. Training of the NN is a global error minimization problem compared to the SA method which applies minimization for each pixel in the image. The SA approach embodies physics explicitly in the equations of the SA model. By contrast, the NN embodies

physics implicitly by establishing numerical relationships between HYDROLIGHT calculated spectra and HYDROLIGHT input parameters such as water column absorption and scattering, r_b, and water depth. Since both methods use radiative transfer models, and both use optimization/minimization, the essential difference focuses on philosophy of implementation.

NEURAL NETWORKS

A neural network is a parallel computing architecture that can be trained by supervised learning to perform nonlinear mappings from one vector space to another. [See Lippman (1987) for an introduction to neural networks, or Haykin (1994) for a more complete treatment.] In the present case we solve a subset of the ocean optics inverse problem by mapping from a multi-dimensional remote sensing reflectance (R_{rs}) vector space into a one-dimensional vector space representing water depth. The processing conducted by each processing element (or neuron) in the network consists of forming a weighted sum of the inputs followed by a nonlinear transfer function to produce an output. The outputs thus produced by one layer of processing elements become the inputs to the next layer in the network. The "intelligence" in the network is contained in the weights that go into forming the sum in each processing element. The proper weight values are established by supervised learning using a training set of input vectors where the corresponding output vector is known. The neural network used in this study is a feed-forward, fully connected net with an input layer, a hidden layer, and an output layer.

Supervised training is accomplished by back propagation, which iteratively presents the spectral data as input and depth values as the corresponding desired output. Back propagation uses a gradient descent search technique to adjust network weights at each iteration to minimize the mean squared error between the desired output (known depth) and the actual network output. The training results in a network that produces estimates of depth given the spectrum of R_{rs}. The network accuracy in general is tested utilizing an independent set of data not included in the training process. In this case the test set is taken from HyMaP imagery.

NEURAL NETWORK TRAINING SET

In Situ hyperspectral absorption and beam attenuation data in the coastal waters of the West Florida Shelf provided water optical properties for a series of HYDROLIGHT runs. These field data were collected at approximately 50 stations ranging from very turbid waters within Tampa Bay to clearer offshore waters. For this paper we focus on bathymetry retrieval over sandy bottoms, therefore, seven sand bottom types (coral sand, Biloxi sand, White bio-turbated sediment (CoBOP), CoBOP sand, Ship island sand, Ship Is. gulf, Ship Is. MS sound) were included in the HYDROLIGHT runs that included depths from 0 to 20 meters, wind speed from 0 to 10 m/s, and solar zenith angles from 10 to 50 degrees. HYDROLIGHT produced R_{rs} data at 5 nm intervals from 402.5 to 747.5 nm (70 wavelengths). To use this data for algorithms for specific sensors, such as the HyMaP system used here, the HYDROLIGHT output spectra were resampled by interpolation to match the center point of the spectral bands of the sensor of interest. No attempt has been made to account for HyMaP bandwidth and spectral response function. The seventy HYDROLIGHT

wavelengths were resampled to 21 bands corresponding to HyMaP channels falling in the 400 to 750 nm range. The neural network training set consisted of 2118 samples. Random noise characteristic of the HyMaP sensor was added to the modeled data. The training vectors were also submitted to Principal Components Analysis (PCA) [See Davis (1986) for an introduction] which reduced the number of bands in the imagery to four while conserving 99.85% of the total variance of the data set.

SEMI-ANALYTICAL MODEL

The semi-analytical model for shallow-water remote sensing simultaneously derives the bottom depth and water-column properties using an optimization approach. This approach takes a series of algebraic equations describing the absorption and scattering effects on the remote-sensing reflectance from the water column and optimizes using a predictor-corrector routine to minimize an error function. Each run in the forward direction produces a modeled spectrum that is matched with the observed spectrum. The error function calculates the root mean square between the observed R_{rs} and the modeled R_{rs} in the ranges 400-675nm and 750-830nm. For each set of R_{rs} values, the optimization program computes the error based on the five unknowns: absorption coefficient of phytoplankton pigment at 440nm, absorption coefficient of gelbstoff and detritus at 440nm, bottom reflectance at 550nm, water column depth, and a scattering factor which combines the particle-backscattering coefficient, viewing-angle information, as well as sea state. If the error statistic is larger than some acceptable tolerance level, the model parameters are adjusted according to the optimization scheme and the forward model is run again.

HyMaP IMAGERY

We apply both methods to two HyMaP hyperspectral images of Ship Is., MS. The HyMaP sensor was flown on 24 September 1999 and 11 May 2000. HyMaP is a 126-channel instrument covering the spectral range 450 to 2500 nm. Signal-to-noise ratios are

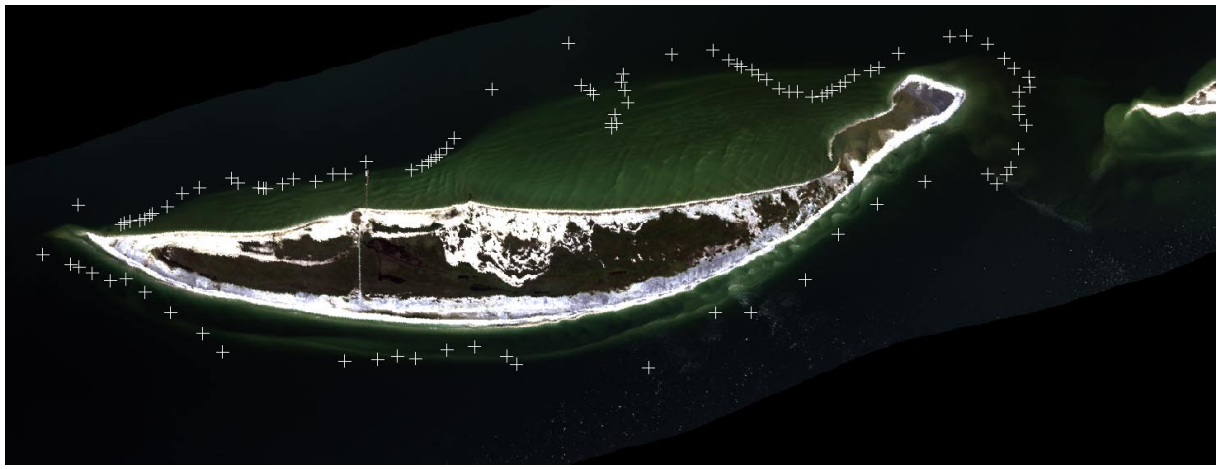

Figure 1 HyMaP image of West Ship Island, MS, 24 Sept. 1999.

500:1 or better in all channels. Analytical Imaging and Geophysics, LLC has calibrated, atmospherically corrected using ATREM (Goetz, *et al.* 1997)), geolocated the imagery, and has converted water-leaving radiance to R_{rs}. Figure 1 is a color rendition of West Ship Island and surrounding shallows made from the HyMaP imagery (24 September 1999). Ground sampling distance for this imagery is 5 m. We used only the first twenty-one HyMaP channels that fall within the 400 to 750 nm range. The ATREM process is intended for land imagery and does not include a correction for skylight reflected from the sea surface. HYDROLIGHT calculates a sky reflectance term which we subtracted from all HyMaP spectra. The white "+" symbols on the image mark the locations of known depths which will serve as ground truth for comparing the methods.

RESULTS

The trained NN with four principal components of noise-corrupted-R_{rs} as input was applied to the HyMaP test set to yield an overall rms error of 1.88 m. In the Ship Is. water we see evidence that bottom reflected light is insignificant in water deeper than 5 m. A more realistic statistic in this case would be to consider rms error in depth retrievals only for those samples in the 0 to 5 m range. In this case the rms error is reduced to 0.88 m.

As a benchmark for evaluating accuracy, we have calculated the rms error of a depth retrieval based on the mid-point of the range. That is, rather than use the NN or SA methods we will estimate the depth to be 2.5 m for all samples. In this case, which we will call the "no skill" method the rms error is 1.10 m. Our NN beats the no skill case.

The SA model is applied to the same test case of HyMaP spectra. It has been shown that the result of an optimization scheme is sensitive to the initial guess. The initial guess for

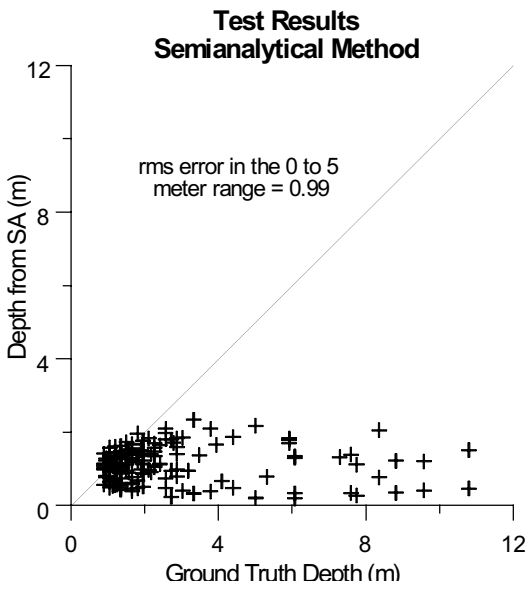

Figure 2

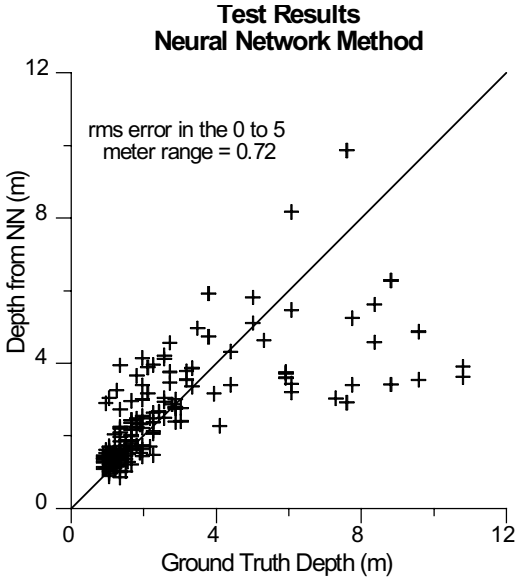

Figure 3

the iteration on each spectrum was chosen by picking characteristic samples from the test set from the image and adjusting the initial guess with respect to these parameters. Once a suitable initial guess was found, it was applied to all test set spectra. The rms error for the SA method is 2.54 m for the entire test set and 0.99 m for depths less than 5 m. Again, as with the neural network the SA method is better than the no skill method but not as good as the NN.

One way to improve the results of both methods is to supply knowledge about bottom reflectance. This can be done easily in this case since the beach in seen in the image. We have taken a pixel near the water (where the sand is believed to be wet) and found the reflectance value at 550 nm to be 0.2. This knowledge is input into the NN by training the NN with a fifth input (bottom reflectance) and then fixing this input at 0.2 when processing the test set. The same information is supplied to the SA method by removing bottom reflectance as a free parameter of the optimization and fixing its value as 0.2 in the model. With bottom reflectance information added, the rms error of the NN method is reduced to 0.72 m and the rms error of the SA method increases to 4.65 m. Figures 2 and 4 show the

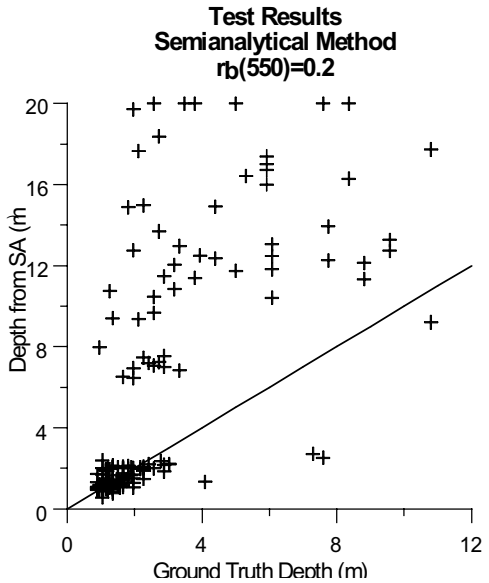

Figure 4

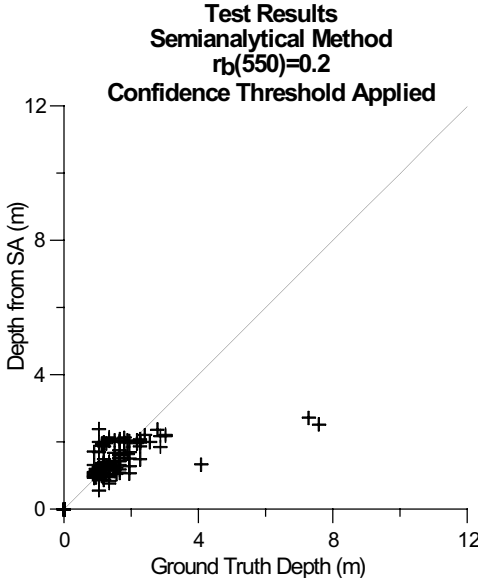

Figure 5

scatter plots of the SA model test set error without and with a fixed bottom reflectance, respectively. Figure 3 shows the scatter plot of the test set error for the NN. With regards to the results of Figure 4, we may attempt to improve the SA performance by introducing a "confidence parameter" to disregard those SA depths that do not have a significant contribution from the ocean bottom or that have some internal inconsistency in the solution. The use of such a parameter may limit the occurrence of outliers noticed in Figure 4; however, it also eliminates many samples where significant bottom reflectance actually occurred. Figure 5 shows the results of excluding low confidence depth retrievals (30% of all test samples excluded including 21% of samples of 0-5m depth).

SUMMARY AND DISCUSSION

The table below provides a summary comparison of the NN and SA methods.

FACTOR	NEURAL NETWORK	SEMI-ANALYTICAL
RTE Model	HYDROLIGHT	Up to 6 parameters (depth, bottom reflectance, absorption of gelbstoff, absorption of chlorophyll, a scattering term, and a spectral bias term)
Data Requirements for Algorithm Development	1)Hyperspectral *in situ* observations of IOPs and bottom reflectance 2)Large number (several thousand) of HYDROLIGHT files for a training set	None.
Potential Optical Complexity	Unlimited, can include fluorescence, Raman scattering, various scattering phase functions, etc.	Restricted by simplified model and by optimization speed and stability when number of parameters is large.
Ancillary Data Required for Algorithm Application	None.	Few estimates of depth, IOPs, and/or bottom reflectance are helpful for an optimization first guess. Solution shows dependency on first guess.
Parameter Optimized	Error in parameter retrieved (depth in this case)	Error in R_{rs} spectrum
Internal confidence measure	No.	Yes.
Parameters Retrieved	The one parameter NN is trained to retrieve.	All model parameters retrieved simultaneously.
Preprocessing of Image Data	NN approach uses PCA to decorrelate and reduce number of spectral bands.	None.
Accuracy of Depth Retrieval On HyMaP Test Images	rms = 0.72 m (0-5m depth, r_b known)	rms = 4.65 m (0-5m depth, r_b known) rms = 0.42 m (0-3m depth, r_b known, confidence threshold applied)

Although each method has its strengths and weakness as summarized in the table, in terms of accuracy of depth retrieval, the NN method has done significantly better for this data set unless a confidence filter has been used to discard many SA retrievals. What would explain this result? Errors in instrument calibration or atmospheric correction would degrade SA performance. However, these factors would also degrade NN performance and would not explain the accuracy difference unless the SA was much more sensitive to these factors than a more forgiving NN. Also one might suspect that there are water constituents in the Mississippi Sound that are not included in the SA model. It is possible that a more complex SA model allowing for additional water constituents would do better, although as the number of parameters in the SA model increases, convergence time and stability are expected to become problems. An examination of the spectral distribution of error in the SA model might help identify any missing constituents in the SA model. We also may have made poor initial guesses in optimization leading to less than optimal retrievals; however, observed variations with initial guess may be addressed with the use of the confidence term. An AVIRIS data set, on which the SA method has performed well in the past, will also be included in future studies to rule out the possibility that some problem might exist with the HyMaP data that is causing problems for the SA method. These factors are the topic of on going research which will lead to a more complete understanding of the characteristics of these methods.

REFERENCES

Davis. John C. *Statistics and Data Analysis in Geology*, Wiley & Sons, Inc., 1986.

Goetz, A.F.H., J.W. Boardman, B. Kindel and K.B. Heidebrecht, "Atmospheric corrections: On deriving surface reflectance from hyperspectral imagers," *Proceedings SPIE Annual Meeting, 3118,* 14-22, 1997.

Haykin, S. *Neural Networks: A Comprehensive Foundation*, Prentice Hall, 1994.

Lippman, R.P., "An introduction to computing with neural nets," *IEEE ASSP Mag.* 4:4-22, 1987.

Lee, Z.P., K.L. Carder, C.D. Mobley, R.G. Steward, and J.S. Patch, "Hyperspectral remote sensing for shallow waters: 2. Deriving bottom depths and water properties by optimization," *Appl. Opt*., 38, 3831-3843, 1999.

Lee, Z.P., K.L. Carder, R.F. Chen, T.G. Peacock, "Properties of the water column and bottom derived from Airborne Visible Infrared Imaging Spectrometer (AVIRIS) data*," J. Geophys. Res.*,Vol. 106 , No. C6 , p. 11,639, 2001.

Mobley, C.D., "*Light and Water: Radiative Transfer in Natural Waters*," Academic Press, 1994.